Neural Stem Cell Mapping with High-Resolution Rapid-Scanning X-Ray Fluorescence Imaging

9

Angela M. Auriat, Helen Nichol, Michael Kelly, and Raphael Guzman

9.1 Introduction

In pre-clinical studies, cell-based therapies improve functional outcome in a variety of diseases of the central nervous system (Chopp et al. 2008). Many different types of stem cells, including bone marrow stromal (BMS) cells, embryonic stem (ES) cells, fetal neural stem (FNS) cells, and umbilical cord blood cells, have been tested (Bliss et al. 2010). Human trials indicate that stem cell treatments are safe and well tolerated (Nelson et al. 2002; Savitz et al. 2005; Kondziolka et al. 2000, 2004, 2005). However, before clinical cell transplantation becomes mainstream, the ideal route and time of delivery, as well as the mechanisms of action need to be identified. Such studies would benefit from serial long-term imaging of transplanted cells with high spatial resolution, sensitivity and functional information. The technique should not impact the therapy, having no influence on cell differentiation, survival, physiology, migration, or mechanisms of action. Additionally, the ideal imaging tool would be able to differentiate viable from dead cells. Several technologies have been used for in vivo neural stem cell imaging, including MRI, positron emission tomography (PET), optical imaging, and single-photon emission computed tomography (SPECT). The relatively high spatial resolution, sensitivity, availability, and lack of

A.M. Auriat, Ph.D. • R. Guzman, M.D. (✉)
Department of Neurosurgery,
Stanford University School of Medicine, Stanford, CA, USA
e-mail: raphaelg@stanford.edu; guzmanr@uhbs.ch

H. Nichol, Ph.D.
Department of Anatomy and Cell Biology,
University of Saskatchewan, Saskatoon, SK, Canada

M. Kelly, M.D., Ph.D.
Department of Neurosurgery,
University of Saskatchewan, Saskatoon, SK, Canada

J. Jolkkonen, P. Walczak (eds.), *Cell-Based Therapies in Stroke*,
DOI 10.1007/978-3-7091-1175-8_9,

ionizing radiation has made MRI one of the most frequently used imaging modalities for in vivo stem cell tracking.

For MR imaging, cells must be preloaded with a contrast agent, such as gadolinium-rhodamine dextran (Modo et al. 2004), superparamagnetic iron oxide (SPIO) (Arbab et al. 2004; Guzman et al. 2007), or ultrasmall superparamagnetic iron oxide (USPIO) particles (Guzman et al. 2008; Bulte et al. 2002). The most common technique for labeling cells is using SPIO in combination with a transfection agent such as Lipofectamine or protamine sulfate. The SPIO strongly affects the T_2 relaxation time, resulting in hypointensities on the MR images. Several studies have used MRI to longitudinally track transplanted iron-labeled cells in different animal models including stroke (Modo et al. 2004; Guzman et al. 2007, 2008; Bulte et al. 2002; Hoehn et al. 2002; Zhang et al. 2003; Franklin et al. 1999). However, if transplanted cells divide or migrate away from each other, the SPIO signal becomes diluted (Berman et al. 2011). In addition, since SPIO is inert it is not destroyed when stem cells die or are phagocytosed by macrophages after transplantation (Bliss et al. 2007). Thus SPIO can be detected with MRI long after all transplanted cells have died (Berman et al. 2011). Moreover, many parts of the brain are naturally rich in paramagnetic iron (ferritin and hemosiderin) which cannot be distinguished from SPIO with MRI. These issues raise concern over the usefulness of long-term MRI tracking of SPIO-labeled cells following transplantation.

Synchrotron rapid-scanning X-ray fluorescence mapping (RS-XRF) can both map and quantify total iron in tissues, but it must be used with discretion. Quantification of iron in individual histological sections will allow for the study of changes in SPIO concentration. The following review will identify the key strengths and weaknesses of using RS-XRF to identify SPIO-labeled stem cells, will outline the current findings, and lastly indicate the future potential for this technology.

9.2 Cell Tracking with SPIO

9.2.1 Issues with Tracking SPIO-Labeled Cells

Cell death and division are two major issues when imaging SPIO-labeled stem cells. In a recent study by the Walczak group, SPIO-labeled stem cells were injected into the brains of immunocompetent and immunodeficient mice (Berman et al. 2011). Serial MR imaging of the transplanted cells showed a more intense and persistent signal detection in the immunocompetent mice, in which no surviving transplanted cells could be identified. Whereas, the immunodeficient mice had a more rapid reduction in MR T2 signal detection over time, corresponding to a rapid proliferation and migration of transplanted cells, which was confirmed with bioluminescence imaging and immunohistochemistry.

There is conflicting evidence regarding the degree of clearance/persistence of SPIO signal following the death of labeled cells. Guzman et al. (2007) showed

that SPIO-labeled NSCs killed with repeated freeze-thaw cycles prior to injection were nearly completely cleared, whereas the living cells injected into the contralateral hemisphere remained detectable. Similar findings were also described when using rodent neural stem cells (Zhang et al. 2003). When SPIO-labeled cells are injected directly into the cisterna magna, no iron-positive cells were detected with Prussian blue staining, suggesting that all iron from the labeled cells is cleared (Zhang et al. 2004). However, other studies have found a persistent MRI signal after the death of transplanted SPIO-labeled cells (Winter et al. 2010; Gonzalez-Lara et al. 2011).

Previous research has shown that some cell lines undergo asymmetric cell division, resulting in a sharp drop-off in SPIO label in one population of cells and not in another (Walczak et al. 2007). In this study, SPIO-labeled C17.2 cells were injected into the lateral ventricle of neonatal shiverer mice; the cells retaining the most SPIO remained at the lateral ventricles, whereas the cells with less SPIO migrated away from the ventricles and rapidly had undetectable levels of iron labeling. Quantification of iron in individual cells with XRF would allow for precise measurements of the loss of iron in migrating cell populations.

MR imaging of SPIO-labeled cells is impaired in injury models with a strong inflammatory response (Vandeputte et al. 2011). In the photothrombotic model of stroke, T2*-weighted images have hypointensities resulting from the accumulation of endogenous iron containing inflammatory cells and glial scar formation at the border of the injury. The images from the non-cell-treated animals were indistinguishable from those treated with SPIO-labeled stem cells (Vandeputte et al. 2011). The combination of RS-XRF and immunohistochemistry could allow for the differential quantification of iron in inflammatory and SPIO-labeled transplanted stem cells.

9.2.2 Tracking Cells After Different Methods of Transplantation

Intravascular and stereotactic cell transplantation are two major methods of stem cell transplantation (Pendharkar et al. 2010). Stereotactic transplantations inject the cells directly into the brain, either parenchyma or intracisternally. Intravascular transplantations inject cells into the periphery either intra-arterially, typically into the blood vesicles supplying the brain, or intravenously. Each transplantation method has a unique pattern of cell distribution and engraftment (Pendharkar et al. 2010). Several studies have compared the different transplantation methods, although generalizations across these studies are difficult as there are differences in injury models, cell type, treatment delay, and other factors that can alter distribution and engraftment results (Auriat et al. 2011). Comparison of intraventricular, intraparenchymal, and intravenous transplantations indicated that the greatest number of cells engrafted in the brain is found following the intraparenchymal injection (Jin et al. 2005). If we compare just the vascular delivery methods, intra-arterial injections have a far greater engraftment of NPCs in the ischemic brain than intravenous

injection (Pendharkar et al. 2010; Li et al. 2010). Similar results have been found after intra-arterial compared to intravenous transplantation of mesenchymal stem cells (Walczak et al. 2008). The differences in engraftment and distribution with different transplantation methods have implications for the ease with which cells can be detected with MRI. SPIO-labeled stem cells, transplanted in a variety of ways, have been identified in the ischemic rat brain with MRI (Guzman et al. 2007; Li et al. 2010; Walczak et al. 2008). However, with diffuse distribution after intravascular delivery, more sensitive monitoring is required. The cellular resolution and high sensitivity of RS-XRF make it ideal for identifying small quantities of iron in SPIO-labeled stem cells.

9.3 Rapid-Scanning X-Ray Fluorescence Mapping

X-ray fluorescence is a quantitative technique for mapping element distribution. Other established techniques can quantify element concentrations at low levels with high accuracy such as inductively coupled plasma mass spectrometry (ICP-MS) and atomic emission spectroscopy (AE). However, these technologies require the isolation and purification of the target structure; this can be a difficult task and may result in contamination artifacts. Recent developments with third-generation synchrotrons, which can generate spatially coherent high-brilliance X-rays, have resulted in the ability to quantify elements nondestructively, allowing for the mapping of elements in hydrated tissue sections and whole cells with high sensitivity and micron resolution (Paunesku et al. 2006). The high sensitivity of this technology, both in terms of localization and quantification, make it ideal for studying iron in transplanted stem cells.

9.3.1 Basic Principles of X-Ray Fluorescence

A tissue slice or whole mount is raster scanned in a collimated beam of hard X-rays having an energy above that needed to eject core-shell electrons from all elements of interest (Fig. 9.1). A higher shell electron fills the electron hole resulting in the emission of a photon equal to the difference in binding energies of the two shells involved. Each binding energy is proportional to the squared nuclear charge, meaning that the emitted photon energy is unique for each element. The emitted photons are detected and used to identify and quantify the elements present in the sample. The X-ray beam can be focused allowing for high-resolution images (Fahrni 2007).

Rapid-scanning X-ray fluorescence mapping (RS-XRF) is a new imaging technique developed at the Stanford Synchrotron Radiation Lightsourse (Popescu et al. 2011). The primary advantage of rapid scanning is that large samples can be mapped in a reasonable time. Emission spectra are collected at each point and by selecting the appropriate energy ranges, multiple elements can be mapped simultaneously. The X-ray fluorescence counts can be further quantified by comparison with XRF standards.

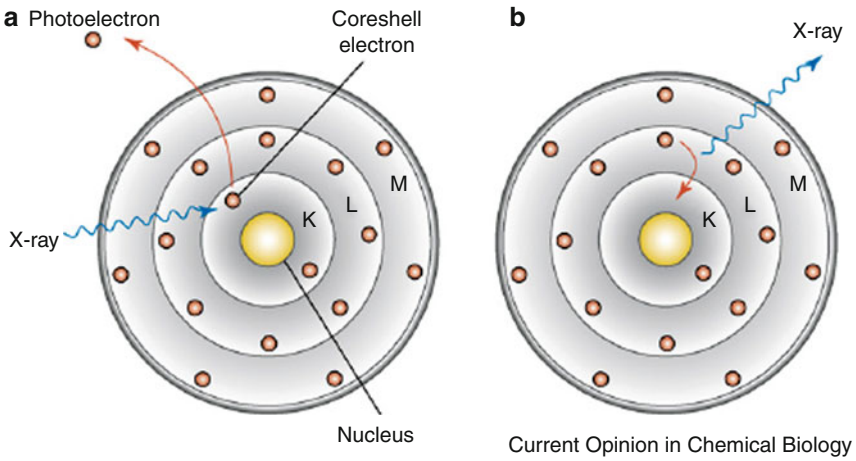

Fig. 9.1 Bohr atom model. X-ray fluorescence imaging involves the excitation of the sample with an X-ray, leading to the ejection of a core-shell electron from the atom (**a**). An electron from a higher shell falls down to fill the electron hole, resulting in the emission of a photon of an energy equal to the difference in binding energies of the two shells involved in the transition (**b**) (Reprinted from Fahrni (2007) with permission from *Current Opinion in Chemical Biology*)

9.3.2 Biological Applications of XRF

Previously, XRF has been used in the mapping of clinical postmortem tissue in various patient populations (Szczerbowska-Boruchowska et al. 2011, 2012) and in animal models (Chwiej et al. 2011). Of particular interest are neurodegenerative diseases, in which irregular distributions of various elements are thought to be important. For instance, abnormal metal distribution of elements such as Cu, Fe, and Zn have been suggested to play a role in neurodegenerative disorders including Alzheimer's disease, Parkinson's disease,and amyotrophic lateral sclerosis. Metal deposits can be nondestructively mapped in brain tissue and individual cells (Tomik et al. 2006; Chwiej et al. 2005; Szczerbowska-Boruchowska et al. 2012), and relationships between metals can be easily identified with colocalization and quantification. Animal models can also be assessed with RS-XRF to identify element distribution following brain injury (Silasi et al. 2012; Auriat et al. 2012). Sensitive mapping and quantification of metals can be particularly useful in the assessment of treatments, such as therapeutic chelators, which alter metal levels in the brain (Auriat et al. 2012; Popescu and Nichol 2011). Quantitative and topographic mapping of element distributions with RS-XRF would be particularly useful for identifying how specific the chelators are as well as how chelation of one metal may alter the distribution of other metals. At the cellular level, XRF has been used to examine the mechanisms of pluripotency and differentiation in embryonic and induced pluripotent stem cells (Cardoso et al. 2011). Elemental maps at the atomic level indicated that phosphorus and sulfur levels rise and consistent patterns of element polarization within the cells are observed during neural differentiation.

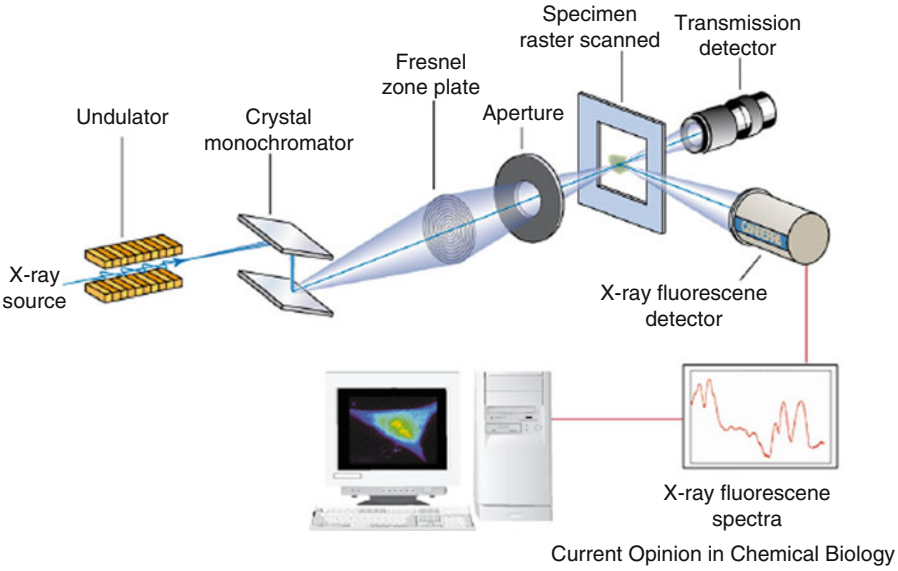

Fig. 9.2 Illustration of one of the typical sample setups used in RS-XRF. The crystal monochromator is used to select the desired X-ray energy, which is then focused with a Fresnal zone plate. Apertures of varying sizes are used to control the spot size of the beam. The sample is moved through the beam; this raster scanning across the area of interest results in a quantitative element map (Reprinted from Fahrni (2007) with permission from *Current Opinion in Chemical Biology*)

9.4 Sample Preparation

The high sensitivity of XRF makes samples highly sensitive to contamination. Throughout the processing of tissue samples, care must be taken to avoid introducing any foreign elements. Solutions used to process samples should be prepared with ultrapure water (Auriat et al. 2012; Hackett MJ et al. 2012). For the study of SPIO-labeled stem cells in tissue, brains can be fixed and cryostat-sectioned using a Teflon-coated blade. Sections should be placed on metal-free plastic coverslips such as Thermanox. Our group has previously imaged blank Thermanox coverslips and found them to be low in all elements of interest for our samples. It is also critical to keep sectioned tissue in an atmosphere free of dust and other contaminants, because any partials on the samples will be observed in the resulting image (Fig. 9.2).

9.5 Cellular Iron Quantification in SPIO-Labeled Stem Cells

Our recent findings indicate that it is possible to use RS-XRF to characterize the migration of SPIO-labeled neural stem cells and to correlate these findings with MRI.

The scanning was completed at the Stanford Synchrotron Radiation Lightsource (SSRL) on beamline 2–3. The 13-keV beam was oriented at 45° to the vertically mounted samples and 90° to the detector. Sections from the injured hemisphere were imaged at up to a 3-μm resolution with a 200-ms dwell time, allowing for the identification of individual cells. Quantification was completed by comparing the signal intensity of the samples to the signal from standards of known concentrations (Micromatters Inc., Sault Ste. Marie, ON, CAN). Analysis of the SPIO-labeled hNPCs at high resolution showed that on average stem cells contained about 7 pg of iron (Fig. 9.3).

The nondestructive nature of RS-XRF imaging means that after imaging, the same sections can be labeled with immunohistochemical markers. Recent advances at SSRL now allow for simultaneous mapping of fluorescent immunohistochemical markers and RS-XRF imaging, facilitating the identification of specific cell types.

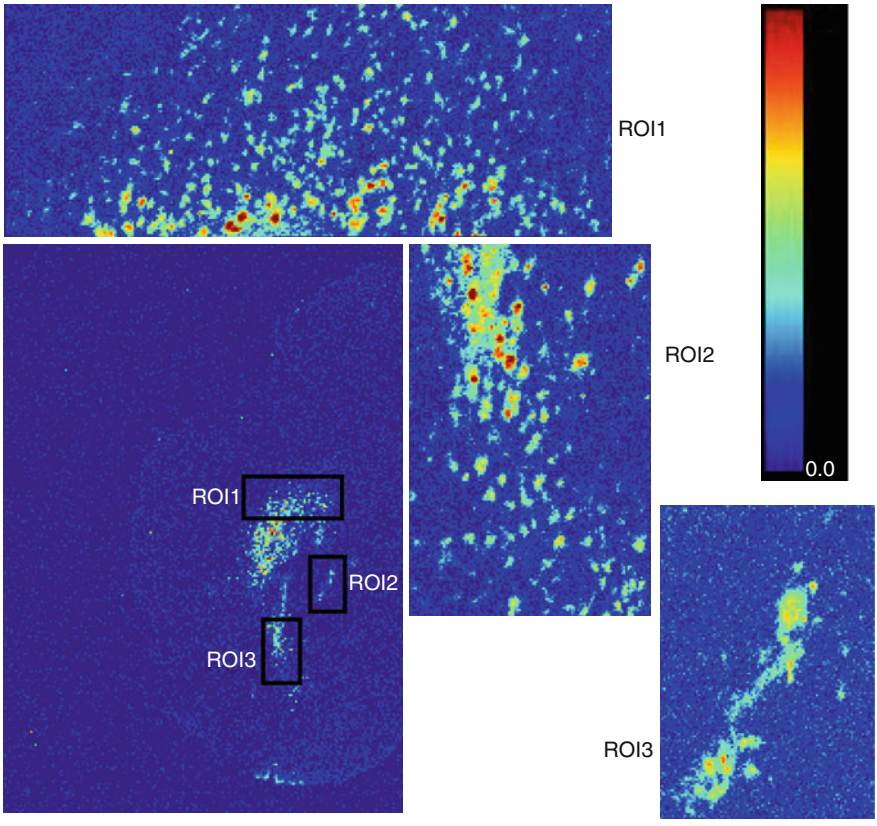

Fig. 9.3 RS-XRF image of SPIO-labeled stem cells injected stereotactically into an ischemic mouse brain. The high-resolution ROI correspond to the areas identified in the ischemic hemisphere. Concentrations of iron are color coded, with red being the highest level and blue being the lowest. The color legend for XRF images represents pg/cm^2 iron

9.6 Future Directions for RS-XRF

The synchrotron rapid-scanning XRF imaged cells at high resolution and allowed for iron quantification in individual cells. These are highly promising results, indicating that XRF will be useful for future studies identifying parameters important to monitoring SPIO-labeled stem cells in vivo. With the ability to accurately map and quantify iron levels in individual cells, it will be possible to determine the concentration of iron in different populations of transplanted stem cells. The development of genetically encoded reporters, whereby specific protein expression causes the formation of suitable contrast agents, will likely be important in future research. Endogenous and persistent generation of cellular contrast would be highly beneficial for studies of stem cell transplantation, ensuring the specific and persistent imaging of surviving cells. Several MRI reporter genes are being developed, including those expressing iron homeostasis proteins such as transferrin receptor (Weissleder et al. 2000) and ferritin (Genove et al. 2005; Cohen et al. 2005), as well as the use of the genes present in magnetotactic bacteria (magA) (Zurkiya et al. 2008; Goldhawk et al. 2009). RS-XRF could play an important role in the development of new reporter genes, accurately quantifying the iron signal in individual cells, helping to ensure that the threshold for MRI detection is met.

References

Arbab AS, Yocum GT, Kalish H, Jordan EK, Anderson SA, Khakoo AY et al (2004) Efficient magnetic cell labeling with protamine sulfate complexed to ferumoxides for cellular mri. Blood 104:1217–1223

Auriat AM, Rosenblum S, Smith TN, Guzman R (2011) Intravascular stem cell transplantation for stroke. Trans Stroke Res 2:250–265

Auriat AM, Silasi G, Wei Z, Paquette R, Paterson P, Nichol H et al (2012) Ferric iron chelation lowers brain iron levels after intracerebral hemorrhage in rats but does not improve outcome. Exp Neurol 234:136–143

Berman SC, Galpoththawela C, Gilad AA, Bulte JW, Walczak P (2011) Long-term mr cell tracking of neural stem cells grafted in immunocompetent versus immunodeficient mice reveals distinct differences in contrast between live and dead cells. Magn Reson Med 65:564–574

Bliss T, Guzman R, Daadi M, Steinberg GK (2007) Cell transplantation therapy for stroke. Stroke 38:817–826

Bliss TM, Andres RH, Steinberg GK (2010) Optimizing the success of cell transplantation therapy for stroke. Neurobiol Dis 37:275–283

Bulte JW, Duncan ID, Frank JA (2002) In vivo magnetic resonance tracking of magnetically labeled cells after transplantation. J Cereb Blood Flow Metab 22:899–907

Cardoso SC, Stelling MP, Paulsen BS, Rehen SK (2011) Synchrotron radiation x-ray microfluorescence reveals polarized distribution of atomic elements during differentiation of pluripotent stem cells. PLoS One 6:e29244

Chopp M, Li Y, Zhang J (2008) Plasticity and remodeling of brain. J Neurol Sci 265:97–101

Chwiej J, Fik-Mazgaj K, Szczerbowska-Boruchowska M, Lankosz M, Ostachowicz J, Adamek D et al (2005) Classification of nerve cells from substantia nigra of patients with parkinson's disease and amyotrophic lateral sclerosis with the use of x-ray fluorescence microscopy and multivariate methods. Anal Chem 77:2895–2900

Chwiej J, Sarapata A, Janeczko K, Stegowski Z, Appel K, Setkowicz Z (2011) X-ray fluorescence analysis of long-term changes in the levels and distributions of trace elements in the rat brain following mechanical injury. J Biol Inorg Chem 16:275–358

Cohen B, Dafni H, Meir G, Harmelin A, Neeman M (2005) Ferritin as an endogenous mri reporter for noninvasive imaging of gene expression in c6 glioma tumors. Neoplasia 7:109–117

Fahrni CJ (2007) Biological applications of x-ray fluorescence microscopy: exploring the subcellular topography and speciation of transition metals. Curr Opin Chem Biol 11:121–127

Franklin RJ, Blaschuk KL, Bearchell MC, Prestoz LL, Setzu A, Brindle KM et al (1999) Magnetic resonance imaging of transplanted oligodendrocyte precursors in the rat brain. Neuroreport 10:3961–3965

Genove G, DeMarco U, Xu H, Goins WF, Ahrens ET (2005) A new transgene reporter for in vivo magnetic resonance imaging. Nat Med 11:450–454

Goldhawk DE, Lemaire C, McCreary CR, McGirr R, Dhanvantari S, Thompson RT et al (2009) Magnetic resonance imaging of cells overexpressing maga, an endogenous contrast agent for live cell imaging. Mol Imaging 8:129–139

Gonzalez-Lara LE, Xu X, Hofstetrova K, Pniak A, Chen Y, McFadden CD et al (2011) The use of cellular magnetic resonance imaging to track the fate of iron-labeled multipotent stromal cells after direct transplantation in a mouse model of spinal cord injury. Mol Imaging Biol 13:702–711

Guzman R, Uchida N, Bliss TM, He D, Christopherson KK, Stellwagen D et al (2007) Long-term monitoring of transplanted human neural stem cells in developmental and pathological contexts with mri. Proc Natl Acad Sci USA 104:10211–10216

Guzman R, Bliss T, De Los Angeles A, Moseley M, Palmer T, Steinberg G (2008) Neural progenitor cells transplanted into the uninjured brain undergo targeted migration after stroke onset. J Neurosci Res 86:873–882

Hackett MJ, Smith SE, Paterson PG, Nichol H, Pickering IJ, George GN (2012) X-ray absorption spectroscopy at the sulfur K-edge: A new tool to investigate the biomedical mechanisms of neurodegeneration. ACS Chem Neurosci 3:178–185

Hoehn M, Kustermann E, Blunk J, Wiedermann D, Trapp T, Wecker S et al (2002) Monitoring of implanted stem cell migration in vivo: a highly resolved in vivo magnetic resonance imaging investigation of experimental stroke in rat. Proc Natl Acad Sci USA 99: 16267–16272

Jin K, Sun Y, Xie L, Mao XO, Childs J, Peel A et al (2005) Comparison of ischemia-directed migration of neural precursor cells after intrastriatal, intraventricular, or intravenous transplantation in the rat. Neurobiol Dis 18:366–374

Kondziolka D, Wechsler L, Goldstein S, Meltzer C, Thulborn KR, Gebel J et al (2000) Transplantation of cultured human neuronal cells for patients with stroke. Neurology 55:565–569

Kondziolka D, Steinberg GK, Cullen SB, McGrogan M (2004) Evaluation of surgical techniques for neuronal cell transplantation used in patients with stroke. Cell Transplant 13:749–754

Kondziolka D, Steinberg GK, Wechsler L, Meltzer CC, Elder E, Gebel J et al (2005) Neurotransplantation for patients with subcortical motor stroke: a phase 2 randomized trial. J Neurosurg 103:38–45

Li L, Jiang Q, Ding G, Zhang L, Zhang ZG, Li Q et al (2010) Effects of administration route on migration and distribution of neural progenitor cells transplanted into rats with focal cerebral ischemia, an mri study. J Cereb Blood Flow Metab 30:653–662

Modo M, Mellodew K, Cash D, Fraser SE, Meade TJ, Price J et al (2004) Mapping transplanted stem cell migration after a stroke: a serial, in vivo magnetic resonance imaging study. Neuroimage 21:311–317

Nelson PT, Kondziolka D, Wechsler L, Goldstein S, Gebel J, DeCesare S et al (2002) Clonal human (hnt) neuron grafts for stroke therapy: neuropathology in a patient 27 months after implantation. Am J Pathol 160:1201–1206

Paunesku T, Vogt S, Maser J, Lai B, Woloschak G (2006) X-ray fluorescence microprobe imaging in biology and medicine. J Cell Biochem 99:1489–1502

Pendharkar AV, Chua JY, Andres RH, Wang N, Gaeta X, Wang H et al (2010) Biodistribution of neural stem cells after intravascular therapy for hypoxic-ischemia. Stroke 41:2064–2070

Popescu BF, Nichol H (2011) Mapping brain metals to evaluate therapies for neurodegenerative disease. CNS Neurosci Ther 17:256–268

Savitz SI, Dinsmore J, Wu J, Henderson GV, Stieg P, Caplan LR (2005) Neurotransplantation of fetal porcine cells in patients with basal ganglia infarcts: a preliminary safety and feasibility study. Cerebrovasc Dis 20:101–107

Silasi G, Klahr AC, Hackett MJ, Auriat AM, Nichol H, Colbourne F (2012) Prolonged therapeutic hypothermia does not adversely impact neuroplasticity after global ischemia in rats. J Cereb Blood Flow Metab 32:1525–1534

Szczerbowska-Boruchowska M, Lankosz M, Adamek D (2011) First step toward the "fingerprinting" of brain tumors based on synchrotron radiation x-ray fluorescence and multiple discriminant analysis. J Biol Inorg Chem 16:1217–1243

Szczerbowska-Boruchowska M, Krygowska-Wajs A, Adamek D (2012) Elemental micro-imaging and quantification of human substantia nigra using synchrotron radiation based x-ray fluorescence-in relation to parkinson's disease. J Phys Condens Matter 24:244104

Tomik B, Chwiej J, Szczerbowska-Boruchowska M, Lankosz M, Wojcik S, Adamek D et al (2006) Implementation of x-ray fluorescence microscopy for investigation of elemental abnormalities in amyotrophic lateral sclerosis. Neurochem Res 31:321–331

Vandeputte C, Thomas D, Dresselaers T, Crabbe A, Verfaillie C, Baekelandt V et al (2011) Characterization of the inflammatory response in a photothrombotic stroke model by mri: implications for stem cell transplantation. Mol Imaging Biol 13:663–671

Walczak P, Kedziorek DA, Gilad AA, Barnett BP, Bulte JW (2007) Applicability and limitations of mr tracking of neural stem cells with asymmetric cell division and rapid turnover: the case of the shiverer dysmyelinated mouse brain. Magn Reson Med 58:261–269

Walczak P, Zhang J, Gilad AA, Kedziorek DA, Ruiz-Cabello J, Young RG et al (2008) Dual-modality monitoring of targeted intraarterial delivery of mesenchymal stem cells after transient ischemia. Stroke 39:1569–1574

Weissleder R, Moore A, Mahmood U, Bhorade R, Benveniste H, Chiocca EA et al (2000) In vivo magnetic resonance imaging of transgene expression. Nat Med 6:351–355

Winter EM, Hogers B, van der Graaf LM, Gittenberger-de Groot AC, Poelmann RE, van der Weerd L (2010) Cell tracking using iron oxide fails to distinguish dead from living transplanted cells in the infarcted heart. Magn Reson Med 63:817–821

Zhang RL, Zhang L, Zhang ZG, Morris D, Jiang Q, Wang L et al (2003) Migration and differentiation of adult rat subventricular zone progenitor cells transplanted into the adult rat striatum. Neuroscience 116:373–382

Zhang Z, Jiang Q, Jiang F, Ding G, Zhang R, Wang L et al (2004) In vivo magnetic resonance imaging tracks adult neural progenitor cell targeting of brain tumor. Neuroimage 23:281–287

Zurkiya O, Chan AW, Hu X (2008) Maga is sufficient for producing magnetic nanoparticles in mammalian cells, making it an mri reporter. Magn Reson Med 59:1225–1231